Modeling and simulation of industrial adiabatic fixed-bed reactor for the catalytic reforming of methane to syngas

M.Taghizadeh Mazandarani , H. Ebrahim

Chemical Engineering Department, Faculty of Engineering, Mazandaran University, P.O.Box:484, Babol, Iran, E-mail: taghizadehfr@yahoo.com , Tel: +98111-3234204, Fax: +98111-3234201

Abstract

An industrial adiabatic fixed-bed reactor for the catalytic reforming of methane to synthesis gas on a commercial supported Ni catalyst at high temperature and pressure (P_{tot} =39 bar, T_g =894 K), is simulated using a steady-state one-dimensional heterogeneous reactor model. Both external concentration and temperature gradients as well as intra-particle concentration gradients are taken into account. The intrinsic kinetics of the reforming and water-gas shift reactions were taken from Numaguchi and Kikuchi (1988).The gas-phase and solid-phase continuity and energy differential equations are solved simultaneously using MATLAB software. In this program the *finite volume* method is used for solving the corresponding continuity equations in solid phase (catalyst). The data taken from the *Khorasan petrochemical company* is applied to the proposed model to perform the simulation and the simulated results are then compared to the experimental data at the outlet of reactor.

Keywords: Simulation, steam reforming, finite volume, adiabatic fixed-bed reactor

1. Introduction

Upgrading of natural gas (rich in methane) into more valuable chemicals, such as synthesis gas (syngas), has been investigated intensively in the past decade. In recent years, hydrogen is considered a clean energy source and its market demand is steadily increasing [1, 2].

Steam reforming of natural gas is widely used to produce syngas, a mixture of hydrogen and carbon monoxide in various proportions [3]. Syngas is used as feedstock in a number of industrial processes such as production of ammonia, methanol synthesis, the Fischer-Tropsch process, and the hydroformylation of olefins [4, 5]. The whole process is endothermic and occurs over a Ni-based catalyst in tubular reactors; equilibrium conditions are quickly reached at high temperature. Although the intensive research efforts have been performed on the kinetics and mechanism of the reaction, the preparation of catalyst and the evaluation of process

and equipment [6, 7], the detailed reactor modeling and simulation of SRM on an industrial scale is required.
In this work an industrial adiabatic fixed-bed reactor for the catalytic reforming of methane to synthesis gas is simulated using a steady-state one-dimensional heterogeneous reactor model.

2. The model

Adiabatic fixed-bed SRM reactor is simulated using a steady-state one-dimensional heterogeneous reactor model. Intra-particle concentration gradients were taken into account explicitly, by solving the continuity equations in the catalyst pellet at each position along the fixed-bed reactor co-ordinate. The reactor designs are based on supported Ni catalysts, which catalyse the formation of synthesis gas via steam reforming followed by water-gas shift reactions. The catalyst particle is assumed to be isothermal: the main transport resistance inside the catalyst pellet is due to mass transfer, even in the case of highly exothermic reactions [8]. The gas-phase and solid-phase continuity and energy equations are presented in Table 1 together with the corresponding initial and boundary conditions as well as Langmuir-Hinshelwood rate equations for reforming, and water-gas shift reactions.

Table 1: Reactor model and reaction rate equations with corresponding boundary conditions

Gas phase		$\frac{dy_i}{dZ}+\frac{k_g \times a_v \times \rho_f}{Q_m}(y_i - y_{i,S}^S)=0$	**(1)**
		$\frac{dT_g}{dZ}+\frac{h_f \times a_V}{Q_m \times c_P}(T_g - T_S)=0$	**(2)**
Solid phase		$T_g - T_S = -\frac{\rho_S \times (1-\varepsilon_B)}{h_f \times a_v}\sum_i R_{W,i}(-\Delta H_{f,i})$	**(3)**
		$\rho_f \frac{D_{e,i}/C_t}{r_p^2 \times X^2}\frac{d}{dX}(X^2 \frac{d}{dX}(\frac{y_{i,S}}{\rho_f}))+R_{W,i}\times\rho_S=0$	**(4)**
Gas-phase boundary conditions	$Z=0$	$C_i = C_i^0, T_g = T_g^0$	**(5)**
Solid-phase boundary conditions	$X=0$	$\frac{d}{dX}(\frac{C_{i,s}}{\rho_f})=0$	**(6)**
	$X=1$	$\rho_f \frac{D_{e,i}}{r_p}\frac{d}{dX}(\frac{C_{i,s}}{\rho_f})_{X=1}=k_g(C_i - C_{i,s}^s)$	**(7)**
	Reaction	**Rate equation [9]**	
	$CH_4 + H_2O \leftrightarrow CO + 3H_2$ $\Delta H_{298}^0 = 206\ kJ/mol$	$r_1 = \frac{k_2^{NK}(p_{CH_4} - p_{H_2}^3 \times p_{CO}/K_{eq,1})}{p_{H_2O}^{0.596}}$	**(8)**
	$CO + H_2O \leftrightarrow CO_2 + H_2$ $\Delta H_{298}^0 = -41\ kJ/mol$	$r_2 = k_3^{NK}(p_{CO} - p_{H_2} \times p_{CO_2}/K_{eq,2})$	**(9)**

The model equations (1)-(4) form a set of differential and algebraic equations. Integration along the reactor co-ordinate was carried out using the MATLAB library routine. The solid-phase continuity equations were solved at each increment of the axial direction by means of the method of finite volume.

4. Simulation results

The reactor and catalyst dimensions, as well as the operating conditions and feed composition taken from the *Khorasan petrochemical company* used to perform the simulation are shown in Table 2.
The calculated axial mole fraction and the catalyst and gas-phase temperature profiles are shown in Figures 1 and 2 respectively.
Figure 3 represents measured and calculated values of gas-phase mole fractions at the outlet of reactor.

Table 2: Reactor and catalyst dimensions, feed composition, and operating conditions

Simulation case	Value
Reactor	
d_r (m_r)	1.2
L_r (m_r)	11
ε_B ($m_g^3.m_r^{-3}$)	0.43
V_r (m^3)	12.44
Q (W)	14100000
Catalyst	
nickel oxide	
ρ_S ($kg.m_P^{-3}$)	2300
d_c (m)	0.016
T_S^0 (K)	1330
$D_{e,i}$ ($m_g^3 \times m_P^{-1} \times S^{-1}$)	0.0029
a_V ($m_P^2 \times m_r^{-3}$)	213.74
G (kg)	16309
V_P (m^3)	7.09
N	3306351
Feed composition (mole fraction)	
CH_4	0.23
H_2O	0.75
H_2	0.02
Operating conditions	
Q_m ($kg.m_r^{-2}.S^{-1}$)	23.03
P_{tot} (bar)	39.25
T_g^0 (K)	894

3. Conclusion

A steady-state, one-dimensional heterogeneous reactor model was used to design adiabatic fixed-bed SRM reactors for synthesis gas production. The reactor designs are based on supported Ni catalysts, which catalyse the formation of synthesis gas via steam reforming followed by water-gas shift reactions. Intra-particle concentration gradients were taken into account explicitly, by solving the corresponding continuity equations at each position along the reactor co-ordinate with the finite volume method. The simulation results concerning the global behavior of SRM reactors are given.

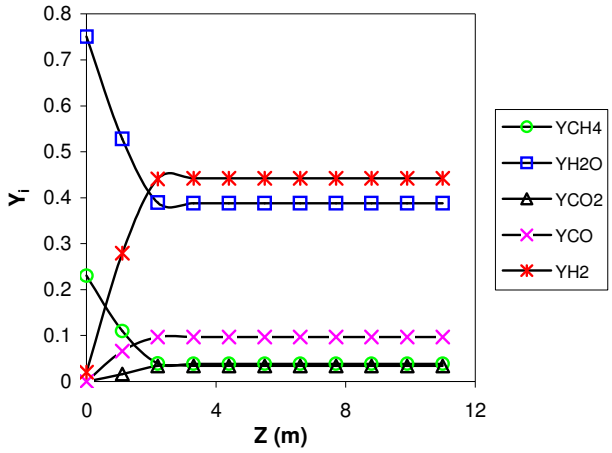

Figure 1: Reactant and product mole fractions vs. axial reactor coordinate.

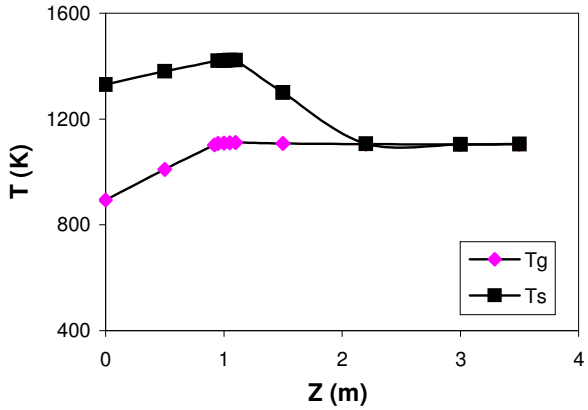

Figure 2: Catalyst and gas-phase temperatures vs. axial reactor coordinate.

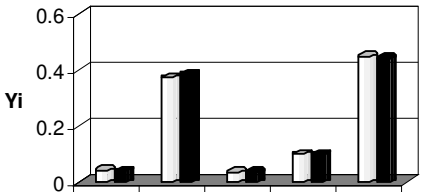

	CH4	H2O	CO2	CO	H2
Experimental data	0.04	0.375	0.035	0.1	0.45
Simulation results	0.039	0.388	0.034	0.097	0.443

Figure 3: Comparison between simulated results and experimental data at the outlet of reactor.

Notation

external pellet surface area per unit reactor volume	$m_P^2.m_r^{-3}$	a_V
specific heat at constant pressure	$J.K_g^{-1}.K^{-1}$	C_P
molar concentration of species i	$mol.m_g^{-3}$	C_i
intra-particle molar concentration of species i	$mol.m_g^{-3}$	$C_{i,S}$
molar concentration of species i, at the external pellet surface	$mol.m_g^{-3}$	$C_{i,S}^S$
effective diffusion coefficient of species i in catalyst	$m_g^3.m_P^{-1}.S^{-1}$	$D_{e,i}$
reactor diameter	mr	d_r
catalyst diameter	m	d_c
total mass of catalyst	kg	G
gas-to-solid heat transfer coefficient	$W.m^{-2}.K^{-1}$	h_f
gas-to-solid mass transfer coefficient	$m_g^3.m_i^{-2}.S^{-1}$	k_g
equilibrium constant of reaction i, reaction dependent	-	$K_{eq,i}$
reactor length	m_r	L_r
partial pressure of component i	bar	P_i
total pressure	bar	P_{tot}
pellet radius	m	r_P
net catalytic production rate of species i per unit catalyst mass	$\frac{m_g^{-4}.K.S}{m_{cat}^{-3}.kg_{cat}}$	$R_{w,i}$
solid temperature	K	T_S
gas-phase temperature	K	T_g
mole fraction of species i	$mol_i.mol_{tot}^{-1}$	y_i
axial reactor co-ordinate	m_r	Z
void fraction of packing	$m_g^3 \times m_r^{-3}$	ε_B
catalyst density	$Kg.m_P^{-3}$	ρ_S
heat rate	**W**	Q
superficial mass flow velocity	$Kg.m_r^{-2}.S^{-1}$	Q_m
dimensionless pellet co-ordinate	-	X

References

[1] F.A. Coutelieris, S. Douvartzides, P. Tsiakaras, (2003) *J. Power Sources*, 123, 200.
[2] R. Peters, R. Dahl, U. K. luttgen, C. Palm, D. Stolten, (2002) *J. Power Sources*, 106, 238.
[3] Armor, J. N., (1999) *Applied Catalysis A*, 176, 159.
[4] Furimsky, E., (1998) *Applied Catalysis A*, 171, 177.
[5] Pena, M. A., Gomez, J. P., & Fierro, J. L. G., (1996) *Applied Catalysis A*, 144, 7.
[6] Xu, J., & Froment, G. F., (1989) *A.I.Ch.E. Journal*, 35, 88.
[7] Berger, R. J., & Marin, G. B., (1999) *Industrial and Engineering Chemistry Research*, 38, 2582.
[8] Froment, G. F., & Bischoff, K. B., (1990) *Chemical reactor analysis and design* (pp. 467–471 and 477–478). London: Wiley.
[9] Numaguchi, T., & Kikuchi, K., (1988) *Chemical Engineering Science*, 43, 2295-2301.